

THE DIVERSITY OF SATURN'S MAIN RINGS: A CASSINI-VIMS PERSPECTIVE. G. Filacchione¹, F. Capaccioni¹, F. Tosi², A. Coradini², P. Cerroni¹, R. N. Clark³, P. D. Nicholson⁴, J. N. Cuzzi⁵, M. H. Hedman⁴, M. R. Showalter⁶, R. Jaumann⁷, K. Stephan⁷, D. P. Cruikshank⁵, R. H. Brown⁸, K. H. Baines⁹, R. M. Nelson⁹, T. B. McCord¹⁰. ¹INAF-IASF, via del Fosso del Cavaliere, 100, 00133, Rome, Italy, gianrico.filacchione@iasf-roma.inaf.it, ²INAF-IFSI, via del Fosso del Cavaliere, 100, 00133, Rome, Italy, ³US Geological Survey, Denver, CO, USA, ⁴Cornell University, Department of Astronomy, Ithaca, NY, USA, ⁵NASA AMES Research Center, Moffett Field, CA, USA, ⁶SETI Institute, Mountain View, CA, USA, ⁷DLR, Berlin, Germany, ⁸Lunar and Planetary Lab, University of Arizona, Tucson, AZ, USA, ⁹Jet Propulsion Laboratory, Pasadena, CA, USA, ¹⁰Space Science Institute NW, Winthrop, WA, USA.

Introduction: In the past years several VIS-NIR spectrophotometric indicators (bands strengths, spectral slopes, continuum levels) were tested on the icy objects of Saturn system in order to derive water ice abundance and grain sizes as well as the distribution of organics contaminants [1, 2]. The method is applied to Cassini-VIMS mosaics of Saturn's main rings to obtain the spatial variability of these physical quantities.

Observations: An East-West mosaic of the rings observed in reflectance acquired by VIMS from 2005-245T22:06 to 2005-246T04:53 in high spatial resolution (VIS IFOV 166x166 μ rad, IR IFOV 250x500 μ rad) with exposure times of 5.12 sec (VIS) and 80 msec (IR) from a distance of about 1.40E6 km from Saturn (inclination angle=16 $^\circ$, phase=51 $^\circ$) is used in this analysis. IR and VIS mosaic images are shown in Fig. 1 and 2 (left panels); the east ansa is partially obscured by the planet's disk shadow. Cassini Division, Encke and Maxwell Gaps are clearly resolved.

Saturnshine: In this observational geometry a portion of the west ansa, mainly across C and B rings, is strongly illuminated by Saturnshine which contaminate at some wavelengths the rings reflectance spectra. To highlight this effect we have mapped the strength of the 1.0 μ m atmospheric band (Fig.1, centre). A similar effect happens also on the east ansa along the shadow's boundary where light transmitted through the upper layer of Saturn's atmosphere falls on the rings.

Composition and size distribution: Saturn rings are mainly composed of water ice particles and organic contaminants [3]; ice abundance is correlated to the the 1.25, 1.5, 2.0 μ m bands strengths which are shown in Fig. 1 (right). Organic contaminants are more difficult to identify because any diagnostic spectral features aren't detected in the VIMS spectral range [4, 5]; however the visible blue slope (0.35-0.52 μ m) allows to derive their distribution across the whole system (Fig. 2, centre). Water ice grain sizes strongly influence both the continuum level at 3.6 μ m and the absorption bands depths. By using the spectral ratio 3.6/1.822 μ m and the 2.0 μ m band strength we evaluate the typical

“regolith” grain sizes by comparison with synthetic ice spectra values [3]. From the resulting scatter-plot of these quantities (Fig. 3) it is possible to derive typical IR spectra and to map their spatial distribution across the rings for different classes of grains in the 10-70 μ m size range.

Acknowledgments: This research was completed thanks to the support of the Italian Space Agency (ASI), Grant ASI/Cassini I/031/05/0.

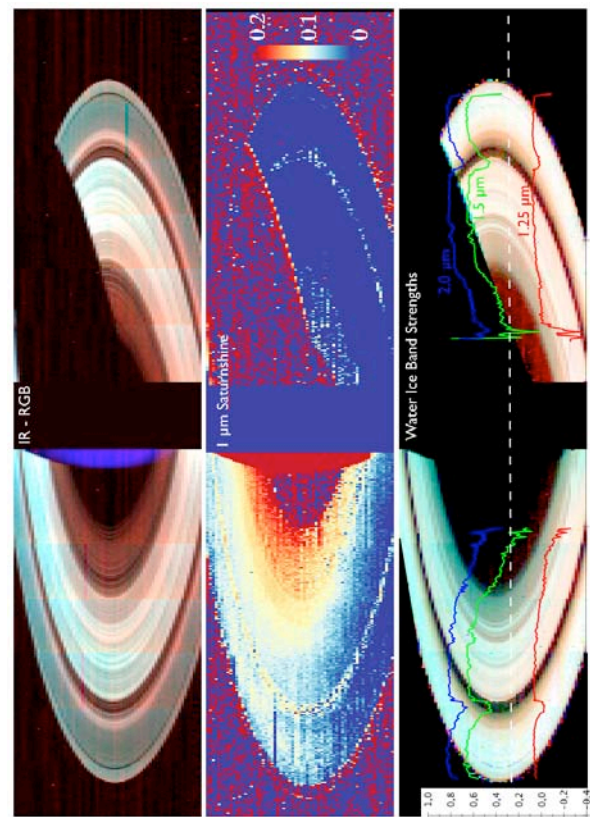


Fig. 1. Left panel: IR mosaic image (B=1.82 μ m, G=2.23 μ m, R=3.6 μ m). Centre: Saturnshine on rings evaluated through the 1.0 μ m band strength. The maximum contamination of Saturn light is in the upper part of the west ansa and along the Saturn's shadow line on the east. Right: color image and radial profiles of the water ice bands strengths (B=2.0 μ m, G=1.5 μ m, R=1.25 μ m).

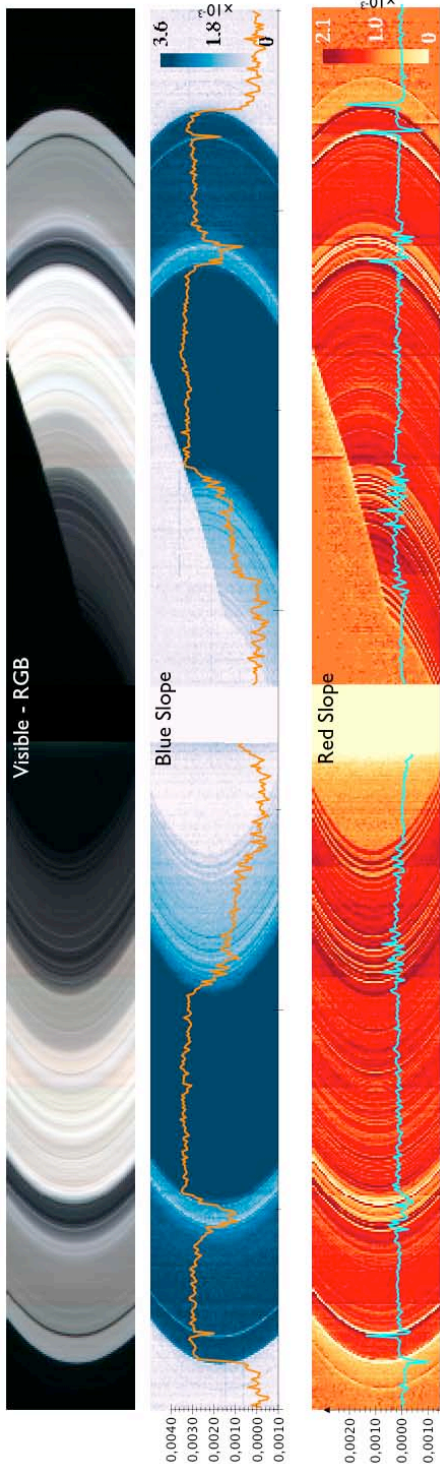


Fig. 2. Left panel: RGB visible mosaic image (B=0.44 μm , G=0.55 μm , R=0.70 μm); Centre: Blue slope (0.35-0.52 μm image and radial profile) is correlated with organic contaminants; Right: Red slope (0.52-0.95 μm image and radial profile) is highly sensitive to radial structures.

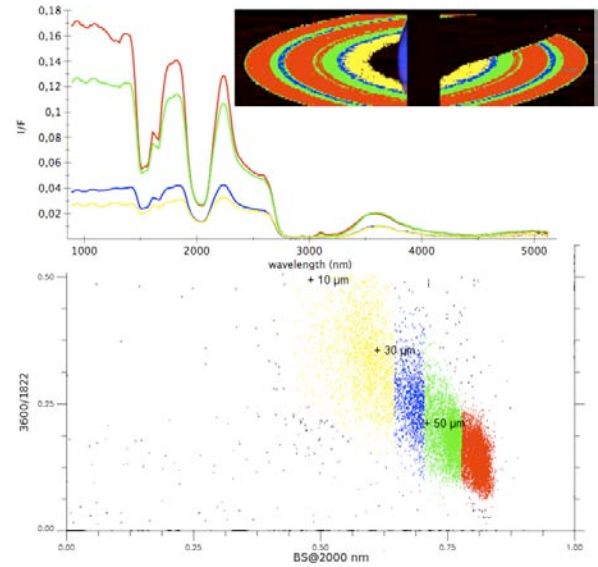


Fig. 3. Bottom panel: 2.0 μm band strength vs 3.6/1.822 μm scatterplot allows to detect both water ice abundance and grain sizes (theoretical positions for 10-30-50 μm water ice grain sizes are indicated). Top: IR mean spectra on 4 distinct classes: 75 μm grains (in red, associated to A and B cores); >50 μm grains (in green, A-in and B-in), <50 μm grains (in blue, Cassini Division and C-out), 30 μm grains (in yellow, C ring).

References: [1] Filacchione, G., Capaccioni, F., McCord, T. B., Coradini, A., Cerroni, P., Bellucci, G., Formisano, V., Brown, R. H., Baines, K. H., Bibring, J. P., Buratti, B. J., Clark, R. N., Combes, M., Cruikshank, D. P., Drossart, P., Jaumann, R., Langevin, Y., Matson, D. L., Mennella, V., Nelson, R. M., Nicholson, P. D., Sicardy, B., Sotin, C., Hansen, G., Hibbitts, K., Showalter, M., Newman, S., D'Aversa, E. (2006), *Icarus*, 186, 259-290. [2] Filacchione, G., Capaccioni, F., Coradini, A., Cerroni, P., Tosi, F., Bellucci, G., Brown, R. H., Baines, K. H., Buratti, B. J., Clark, R. N., Nicholson, P. D., Nelson, R. M., Cuzzi, J. N., McCord, T. B., Hedmann, M. H., Showalter, M. R. (2007), *38th Lunar and Planetary Science Conference*, 1338, 1513. [3] Nicholson, P. D., Hedman, M. M., Clark, R. N., Showalter, M., R., Cruikshank, D. P., Cuzzi, J. N., Filacchione, G., Capaccioni, F., Cerroni, G., Hansen, P., Sicardy, B., Drossart, P., Brown, R. H., Buratti, B., Baines, K., Coradini, A. (2008), *Icarus*, 193, 182-212. [4] Poulet, F., Cuzzi, J. N., French, R. G., Dones, L. (2002), *Icarus* 158, 224-248. [5] Poulet, F., Cruikshank, D. P., Cuzzi, J. N., Roush, T. L., French, R. G. (2003), *Astronomy & Astrophysics*, 412, 305-316.